



1 Interference from alkenes in chemiluminescent NO_x 2 measurements

3
4 Mohammed S. Alam¹, Leigh R. Crilley^{1#}, James D. Lee², Louisa J. Kramer¹,
5 Christian Pfrang¹, Mónica Vázquez-Moreno^{3*}, Amalia Muñoz³, Milagros
6 Ródenas³ and William J. Bloss¹

7
8 ¹ School of Geography, Earth and Environmental Sciences, University of Birmingham, Birmingham, UK

9 ² National Centre for Atmospheric Science, Wolfson Atmospheric Chemistry Laboratories, University of York,
10 York, UK;

11 ³ EUPHORE, Fundación CEAM, Valencia, Spain

12
13 # now at: Department of Chemistry, York University, Toronto, ON, Canada

14 * now at: FISABIO, Valencia, Spain

15
16 Correspondence to: m.s.alam@bham.ac.uk

17 18 **ABSTRACT**

19
20 Nitrogen oxides (NO_x = NO + NO₂) are critical intermediates in atmospheric chemistry. NO_x levels
21 control the cycling and hence abundance of the primary atmospheric oxidants OH and NO₃, and regulate
22 the ozone production which results from the degradation of volatile organic compounds (VOCs) in the
23 presence of sunlight. They are also atmospheric pollutants, and NO₂ is commonly included in air quality
24 objectives and regulations. NO_x levels also affect the production of the nitrate component of secondary
25 aerosol particles and other pollutants such as the lachrymator peroxyacetyl nitrate (PAN). The accurate
26 measurement of NO and NO₂ is therefore crucial to air quality monitoring and understanding
27 atmospheric composition. The most commonly used approach for measurement of NO is
28 chemiluminescent detection of electronically excited NO₂ (NO₂^{*}) from the NO + O₃ reaction. Alkenes,
29 ubiquitous in the atmosphere from biogenic and anthropogenic sources, also react with ozone to produce
30 chemiluminescence and thus may contribute to the measured NO_x signal. Their ozonolysis reaction
31 may also be sufficiently rapid that their abundance in the instrument background cycle, which also
32 utilises reaction with ozone, differs from the measurement cycle – such that the background subtraction
33 is incomplete, and an interference effect results. This interference has been noted previously, and indeed
34 the effect has been used to measure both alkenes and ozone in the atmosphere. Here we report the results
35 of a systematic investigation of the response of a selection of commercial NO_x monitors, ranging from
36 systems used for routine air quality monitoring to atmospheric research instrumentation, to a series of
37 alkenes. Alkenes investigated range from short chain alkenes, such as ethene, to the biogenic
38 monoterpenes. Experiments were performed in the European Photoreactor (EUPHORE) to ensure
39 common calibration and samples for the monitors, and to unequivocally confirm the alkene levels
40 present (via FTIR). The instrument interference responses ranged from negligible levels up to 11 %
41 depending upon the alkene present and conditions used (*e.g.* presence of co-reactants and differing
42 humidity). Such interferences may be of substantial importance for the interpretation of ambient NO_x
43 data, particularly for high-VOC, low-NO_x environments such as forests, or indoor environments where
44 alkene abundance from personal care and cleaning products may be significant.

45
46



47

48 INTRODUCTION

49

50 Measurement of atmospheric trace constituents is central to atmospheric chemistry research and air
51 pollution monitoring. Key challenges to trace measurements are sensitivity, reactivity and selectivity
52 – as many components of interest are only present at ppb (parts per billion, 10^{-9}) or ppt (parts per trillion,
53 10^{-12}) mixing ratios; in many cases their inherent reactivity necessitates *in situ* detection, and as
54 atmospheric trace composition comprises many thousands of different chemical components (Goldstein
55 and Galbally, 2007). Consequently, specific measurement approaches have been developed to measure
56 key atmospheric species, within the specific conditions (analyte abundance, presence of other
57 constituents) anticipated (Heard, 2008). This paper reports a systematic study of the interference arising
58 in measurements of the nitrogen oxides from the presence of alkenes in sampled air, when using the
59 most widespread air quality monitoring technique of chemiluminescence detection.

60

61 NO_x (= $\text{NO} + \text{NO}_2$) abundance controls the cycling and hence abundance of the primary atmospheric
62 oxidants, hydroxyl (OH) and nitrate (NO_3) radicals, and regulates the ozone production which results
63 from the degradation of volatile organic compounds (VOCs) in sunlight. NO_x are also atmospheric
64 pollutants in their own right, and NO_2 is commonly included in air quality objectives and regulations
65 (as the more harmful component of NO_x) (European Environment Agency, 2018; Chaloulakou et al.
66 (2008). In addition to their role in controlling ozone formation, NO_x levels affect the production of
67 other pollutants such as the lachrymator peroxyacetyl nitrate (PAN), and the nitrate component of
68 secondary aerosol particles. Consequently, accurate measurement of nitrogen oxides in the atmosphere
69 is of major importance for monitoring pollution levels and assessing consequent health impacts, and
70 understanding atmospheric chemical processing. Atmospheric NO and NO_2 are formed from natural
71 processes (lightning, soil emissions of NO, biomass burning and even snowpack emissions) and
72 anthropogenic activities (high temperature combustion in air leading to the breakdown of N_2 and O_2
73 and NO_x production via the Zeldovitch mechanism), where road traffic is the predominant source in
74 many urban areas (Keuken *et al.*, 2009; Grice *et al.*, 2009; Carslaw and Rhys-Tyler, 2013).
75 Consequently, boundary layer NO_x abundance varies over many orders of magnitude – from sub 5-ppt
76 levels in the remote marine boundary layer, to ppm levels in some urban environments (Crawford *et*
77 *al.*, 1997).

78

79 Techniques used for the measurement of atmospheric NO_x include laser-induced fluorescence
80 spectroscopy (LIF), for both NO and NO_2 ; absorption spectroscopy (long-path and cavity-enhanced
81 differential optical absorption spectroscopy, LP- and CE-DOAS, cavity attenuated phase shift
82 spectroscopy (CAPS) and passive diffusion tubes, primarily for NO_2), chemical ionisation mass
83 spectrometry (CIMS) and both on- and offline wet chemical methods *e.g.* long path absorption
84 photometer (LOPAP) (Heard, 2008; Sandholm et al. 1990; Kasyutich et al. 2003; Keabian et al. 2005;
85 Cape, 2009; Fuchs et al. 2009; Villena et al. 2011). However, the most commonly employed technique
86 for the measurement of NO_x species, including for statutory air quality monitoring purposes, is the
87 detection of the chemiluminescence arising from electronically excited NO_2 (NO_2^*) formed from the
88 reaction between NO and O_3 (via R1):

89

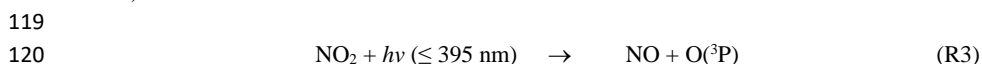


92



93 Chemiluminescent instruments mix sampled ambient air with a reagent stream containing an excess of
94 ozone, to promote the chemiluminescent reaction; the resulting emission signal is measured using a
95 photomultiplier tube (PMT), and consists of contributions from NO_2^* formed as above, but also
96 potentially from other chemiluminescence processes, detector dark counts and other noise
97 contributions. Contributions to the measured emission from other species are minimised by using a red
98 filter on the detector to block emission wavelengths below ca. 600 nm, and by employing a background
99 subtraction cycle: chemiluminescent NO_x monitors commonly acquire a background by increasing the
100 reaction time between NO (from the sampled air) and O_3 (reagent formed within the instrument), using
101 a pre-reactor volume, such that nearly all of the NO present (specifications typically state, in excess of
102 99%) is converted to NO_2 . The difference in PMT signals between the “online” and “background”
103 signals is then taken to be proportional to the NO present in the air sample, following the assumption
104 that the abundance of other species which may contribute to the measured signal is not affected by the
105 background cycle.

106
107 Chemiluminescent instruments typically alternate between two operation modes – one that directly
108 measures NO and one that measures $\Sigma(\text{NO} + \text{NO}_2)$, by first converting NO_2 to NO. The difference
109 between the two values determines the NO_2 mixing ratio (if only NO and NO_2 are present). This is most
110 commonly achieved using a molybdenum (Mo) catalyst heated to 300 – 350°C. However, the reduction
111 of other NO_z species to NO have led to the use of these catalysts in chemiluminescent NO_y monitors to
112 measure total reactive nitrogen rather than NO_2 ($\text{NO}_y = \text{NO}_z + \text{NO}_x$; and $\text{NO}_z =$ other reactive nitrogen
113 species catalysed by Mo convertors *e.g.* HNO_3 , HONO, N_2O_5 , HO_2NO_2 , PAN, NO_3 , organic nitrates –
114 but not NH_3) (Navas *et al.*, 1997; Murphy *et al.*, 2007). If atmospheric mixing ratios of NO_z species are
115 high relative to NO_2 then NO_2 measurements with monitors equipped with Mo catalysts are increasingly
116 inaccurate. This has led to the adoption of photolytic NO_2 conversion stages in research instruments,
117 where a blue light LED convertor is illuminated in a photolysis cell converting NO_2 to NO (Lee *et al.*,
118 2015).



121
122 The photolytic conversion technique can have greater specificity than the heated Mo catalyst as the
123 photolysis wavelengths may be selected to match the NO_2 photolysis action spectrum, while potential
124 NO_z interferences for an NO_2 measurement are thermally unstable and may convert to NO_2 when exposed
125 to heat in the latter approach (Heard, 2008). Despite this, the chemiluminescent analyser with the heated
126 Mo catalyst is the most widely used technique for air quality monitoring of NO and NO_2 worldwide. It
127 is the reference method of measurement specified in the EU directive (BS EN 14211, 2012), providing
128 real-time data with short time resolution for 212 monitoring sites, including kerbside, roadside, urban
129 background, industrial and rural locations (Air Quality Expert Group, 2004).

130 Origins of interferences in chemiluminescent NO_x measurements

131
132 While NO_x measurements are sometimes perceived to be straightforward and routine, in practice a
133 number of factors are known to affect the accuracy of the levels obtained using chemiluminescence
134 approaches. A detailed account of factors affecting atmospheric NO_x measurement overall is given
135 elsewhere (*e.g.* Gerboles *et al.*, 2003; Villena *et al.*, 2012; Reed *et al.*, 2016); here we do not focus upon
136 surface sources/losses but rather upon chemical interferences in chemiluminescent NO_x analysers,
137 which may arise from the following possible general mechanisms:
138
139



- 140 1. Collisional quenching of NO_2^* by an interferent species with a greater collisional efficiency
141 than the bath gas (e.g. air) used for calibration (typically a negative interference, although the
142 magnitude and sign of this depends upon the calibration conditions employed)
- 143 2. Conversion of other N-containing species to NO_x within the NO_2 conversion unit (positive
144 interference)
- 145 3. Chemical removal or interconversion of NO and/or NO_2 by an interferent species generated
146 within the instrument (positive or negative interference)
- 147 4. Chemiluminescence of other chemical species, which is not fully accounted for during the
148 instrument background cycle (positive interference)
- 149

150 Collisional quenching of excited species, mechanism (1), results in a reduction in the
151 chemiluminescence intensity, to an extent dependent upon the pressure, and quenching efficiency – the
152 efficacy with which the quenching species may accept or remove energy from the excited moiety. In
153 the case of electronically excited NO_2 , effective quenching agents have been shown to include H_2O ,
154 CO_2 , H_2 and hydrocarbons (Matthews *et al.*, 1977; Gerboles *et al.*, 2003; Dillon and Crowley, 2018),
155 of which only quenching by water vapour is considered to be significant under most common (ambient
156 air) conditions – sensitivity reductions of up to 8 % have been reported (Steinbacher *et al.*, 2007).
157 Mechanism (2), conversion of other nitrogen-containing species to NO, alongside NO_2 , is a recognised
158 issue with heated Mo converters – interferences between 18 – 100 % have been reported for species
159 such as HONO, HNO_3 , PAN, alkyl nitrates and N_2O_5 (Dunlea *et al.*, 2007; Lamsal *et al.*, 2008). To
160 address these uncertainties, photolytic converters are now commonly employed in research
161 measurements, although for most routine air quality monitoring, heated Mo converters are still
162 employed. Recently, it has been shown that a further interference can arise within the photolytic
163 converter stage – from the generation of HO_x radicals through photolysis of photolabile carbonyl species
164 such as glyoxal, forming peroxy radicals promoting NO-to- NO_2 conversion within the instrument
165 (Villena *et al.*, 2012), resulting in a negative NO_2 interference, which may (under some conditions)
166 exceed the positive interference from retrieval of NO_x species associated with heated Mo converter
167 instruments i.e. mechanism (3).

168
169 The focus of this work relates to mechanism (4): interference in chemiluminescent measurements of
170 NO and NO_2 (using both catalytic and photolytic converters) arising from the chemiluminescence of
171 alkenes in the presence of ozone. Alkene-ozone reactions have received substantial attention as a dark
172 source of HO_x radicals, and a route to the formation of semi-volatile compounds which contribute to
173 secondary organic aerosol (SOA), particularly for biogenic alkenes such as isoprene and the mono- and
174 sesquiterpenes (e.g. Johnson & Marston, 2008; Shrivastava *et al.*, 2017). Rate constants for ozonolysis
175 reactions depend on alkene structure, and are typically larger for biogenic alkenes. Chemiluminescence
176 from ozonolysis reactions was first reported by Finlayson *et al.* (1974), and indeed has been used to
177 perform field measurements of both ozone and alkenes (e.g. Velasco *et al.*, 2007; Hills and Zimmerman,
178 1990). This combination – of alkene-ozone reactions giving rise to a chemiluminescent interference
179 signal, and alkene-ozone reactions being sufficiently rapid that alkenes can be appreciably consumed
180 in the background (pre-reactor) cycle, and hence the interference contribution not fully subtracted
181 during the background correction – gives rise to the potential for interference in NO_x measurements,
182 which is the focus of this study.

183
184
185
186
187



188 **EXPERIMENTAL APPROACH**

189

190 Experiments were performed using chamber A of the two 200m³ simulation chambers of the European
191 Photoreactor (EUPHORE) facility in Valencia, Spain to provide a common, homogeneous air volume
192 for multiple NO_x analysers to sample from. The EUPHORE chambers are formed from fluorine-ethene-
193 propene (FEP) Teflon foil fitted with housings that exclude ambient light (Wiesen, 2001; Munoz *et al.*,
194 2011). The chambers are fitted with large horizontal and vertical fans to ensure rapid mixing (timescale
195 3 minutes). Instrumentation used comprised long-path FTIR (for absolute and specific alkene / VOC
196 measurements), monitors for temperature, pressure, humidity (dew-point hygrometer), ozone (UV
197 absorption) and CO (infrared absorption). NO_x levels were measured using four independent
198 chemiluminescent monitors, plus (in the case of NO₂) LP-DOAS absorption spectroscopy – All monitor
199 sampling lines were attached to one inlet sampling from the centre of the chamber.

200

201 Monitors 1 and 2 employed heated Mo catalysts, while 3 and 4 used photolytic NO₂ converters (see
202 Table 1). All NO_x monitors were calibrated at the start and end of the two-week measurement period
203 using a multi-point calibration derived from a primary NO standard (BOC 5ppm alpha standard,
204 certified to the NPL scale) in addition to single-point calibrations performed on a daily basis. NO₂
205 calibration was achieved via gas-phase titration using added ozone within the chamber. In some
206 experiments the calibrations and interference were confirmed with use of the EUPHORE long-path
207 DOAS system to unequivocally identify and quantify NO₂.

208

209 All experiments were performed with the chamber housing closed (i.e. dark conditions, $j(\text{NO}_2) < 2 \times 10^{-6}$
210 s^{-1}), at near atmospheric pressure and ambient temperature. For most experiments, humidity was low
211 (dew point ca. -45 °C). The experimental procedure, starting with a clean flushed chamber, was to add
212 SF₆ (as a dilution tracer), followed by successive aliquots of various alkenes and in certain cases
213 additional species (H₂O and CO), whilst recording the measured NO and NO₂ levels, over periods of 1-
214 3 hours. For some systems, ozone was added at the end of the experiment – under such dark, high O₃
215 conditions we can be confident that negligible NO could actually be present in the chamber (e.g. from
216 wall sources) and hence that any “NO” signal observed by the monitors was unequivocally an
217 interference response (as any NO remaining would be rapidly consumed by reaction with O₃). The
218 potential interferant species investigated were *cis*-2-butene (C2B), *trans*-2-butene (T2B), tetra-methyl
219 ethylene (2,3-dimethyl-butene or TME), α -terpinene, limonene, methyl chavicol (estragole) and
220 terpinolene, with 4 – 5 additions of 20 – 50 ppb in each case, together with single- or dual-point
221 interference measurements for ethene, propene, isobutene, isoprene, α -pinene, β -pinene and myrcene.
222 Repeat experiments were performed for *trans*-2-butene, terpinolene and α -terpinene under conditions
223 of increased humidity (up to ca. 30% RH). Alkene mixing ratios introduced into the chamber are given
224 in Table S1. Propene, *cis*-2-butene and *trans*-2-butene where supplied by The Linde Group (purity
225 > 99%); isobutene (purity > 99%) and terpinolene (purity > 85%) from Fluka Analytical; and TME
226 (purity > 98%), isoprene (purity > 99%), limonene (purity > 97%), α -pinene (purity > 97%), β -pinene
227 (purity > 97%), α -terpinene (purity > 85%), estragole (purity > 98%) and myrcene (purity > 99%) from
228 Sigma Aldrich. All reagents were used as supplied.

229

230 Data Analysis

231

232 The limit of detection (LOD) for each instrument was determined under the actual experimental
233 conditions, as three times the standard deviation of the NO and NO₂ signal recorded each day from the
234 empty chamber prior to the start of experiments (*i.e.* before addition of any reactants). The mean LODs



235 determined for NO and NO₂ are shown in Table 1. These LOD values are higher than those quoted by
236 the manufacturers for monitors 1-4 (typically 2-100 ppt) but accurately reflect the actual performance
237 of the instruments as used during these experiments. In the analysis which follows, in order to confirm
238 that any change in measured NO and NO₂ mixing ratio for each alkene addition was not due to noise or
239 drift and therefore signal, the readings were compared to the experimentally determined LOD for each
240 instrument. Only if the measured change was greater than the experimentally determined LOD were
241 these readings used for determining an interference. The interference due to the VOC was determined
242 by means of linear regression (least squares fit), with slopes and their uncertainty and Pearson's
243 correlation coefficients calculated in IGOR (see Tables 2 and 3).

244

245

246 RESULTS

247 Figures 1-3 give the measured VOC mixing ratios and the retrieved "NO" and "NO₂" measurements by
248 the four monitors during the experiment for selected alkenes, along with the regression analysis for
249 determining the interference levels. Spikes in NO and NO₂ mixing ratios observed after an alkene
250 addition (*e.g.* Figure 3) arise from sampling close to the addition point prior to the initial period of
251 mixing in the chamber (~ 3 min) and were disregarded in the analysis. The slow decay of alkene and
252 "NO_x" mixing ratios following each addition arises from dilution effects ($\sim 5.7 \times 10^{-5} \text{ s}^{-1}$, derived from
253 the decay of SF₆).

254 From Figures 1-3, a clear and systematic response from the monitors to the presence of α -terpinene,
255 terpinolene and trans-2-butene was observed, with the magnitude varying between the monitors. In
256 addition to the alkenes in Figures 1-3, significant interference effects were also observed for cis-2-
257 butene, TME and limonene for some of the monitors, as summarised in Tables 2 and 3. No interference
258 was observed, within detection uncertainty, for ethene, propene, isobutene, α -pinene, β -pinene,
259 myrcene or methyl chavicol in any of the monitors. For isoprene, no statistically significant interference
260 was observed for monitors 1-3, while monitor 4 observed a very small positive interference of $0.035 \pm$
261 0.001% (NO channel) and $0.076 \pm 0.002\%$ (NO₂ channel).

262

263 For the alkenes where significant interference was observed, in general a positive interference was
264 observed for NO and a negative interference for NO₂ by monitors 1-4 (Tables 2 and 3), with the
265 exception of TME, where a negative NO interference was observed by monitor 3 (and is discussed
266 later). Generally, for monitor 4 a positive NO interference, and a mixture of both positive and negative
267 NO₂ interferences, was observed. Overall, while the magnitude of interference differed between the
268 monitors, the same trend in the interference was observed, with α -terpinene having the largest
269 interference effect, followed by terpinolene, TME/trans-2-butene, cis-2-butene and limonene.

270

271 The addition of water (RH ca. 30%) led to the observed NO and NO₂ interference for trans-2-butene,
272 terpinolene and α -terpinene decreasing by 30 – 60% as shown in Tables 2 and 3. The addition of CO
273 resulted in an increase in the NO interference observed for TME from below the LOD to 0.7% for
274 monitors 1 and 2 while monitors 3 and 4 exhibited a larger interference increase (Table 2).

275

276 DISCUSSION

277

278 Interference effects on retrieved NO abundance

279



280 Positive NO interferences were observed for those alkenes which react most rapidly with ozone, and
281 hence will be present within the monitor reaction chamber at different levels in the measurement and
282 background modes. This interference is attributed to chemiluminescent emission following the alkene-
283 ozone reaction, and may be attributed to a combination of two factors: formation of excited products in
284 the alkene-ozone reaction which emit chemiluminescence, coupled with the significant removal of some
285 alkenes during the instrument background phase compared with the measurement phase, through their
286 reaction with (elevated levels of) ozone within the instrument, *i.e.* mechanism (4) outlined above.

287
288 Possible origins of this signal are the production of excited HCHO, vibrationally excited OH and
289 electronically excited OH (*e.g.* Finlayson *et al.*, 1974). While the long-pass filters used in
290 chemiluminescence NO_x monitors should preclude emission from electronically excited species,
291 vibrationally excited OH produced through the hydroperoxide mechanism is known to emit in the 700
292 – 1100 nm wavelength range (Finlayson *et al.*, 1974; Schurath *et al.*, 1976; Hansen *et al.*, 1977; Toby,
293 1984), and would be detected as NO₂.

294
295 The difference in the interference effect among monitors may then reflect differences in the conditions
296 (ozone abundance, pressure, residence time) within the reaction cell and filter specifications. The
297 relative magnitudes of the positive interference signals observed between the different monitors are
298 consistent with this picture, as the reaction chamber pressure is much lower for monitors 3 and 4 (*ca.* 1
299 – 10 Torr) compared with monitors 1 and 2 (*ca.* 300 Torr) leading to greater collisional quenching.
300 Similarly, addition of H₂O, which would be expected to efficiently accept vibrational energy from OH
301 radicals (Gerboles *et al.*, 2003), was found to substantially reduce the apparent interference. In the
302 experiments with higher humidity, a reduced interference (factor of *ca.* 2, see Table 2) was observed
303 for all NO experiments for all instruments except for TME for the photolytic converters, where an
304 increase was observed. There is currently no recommended relative humidity in which calibrations
305 should be performed for any of the instruments or within EU and EPA guidelines (AQEG, 2004;
306 USEPA, 2002). However, the installation of permeation driers at the sample inlet should (in principle)
307 reduce the impact of different H₂O / relative humidity levels upon quenching of NO₂ or other species
308 and are a common feature of most modern samplers (AQEG, 2004).

309

310

311 Interference magnitude: kinetic and structural effects

312

313 The most significant effects are the large positive NO interferences observed for the monoterpenes; α -
314 terpinene and terpinolene, within monitors 1, 3 and 4. The criteria for an alkene to display such a
315 positive interference (*i.e.* via mechanism 4) is that it reacts with ozone to produce suitable excited
316 products which exhibit a chemiluminescent signal at appropriate wavelengths. In addition, the alkene
317 must have a sufficiently rapid reaction with ozone that its mixing ratio is substantially reduced during
318 the instrument background phase compared with the measurement phase, precluding the correct
319 subtraction of the interference signal. The reaction rate constants for many alkenes with ozone are well
320 known, allowing the calculation of a kinetic interference potential (KIP) ranking for this second factor
321 (see Supplementary Information for calculation details). The calculated KIP are shown in Table 4 as
322 the percentage of a given alkene's potential chemiluminescent signal which would *not* be subtracted in
323 the standard background cycle, under the assumption that the background cycle conditions (O₃ mixing
324 ratio, residence time) would be sufficient to remove 99% of NO present.

325

326 This ranking does not reflect the precise (relative) interference which is observed, as it neglects
327 structural features which will affect the product yield (and state *i.e.* electronic or vibrationally excited)



328 of the chemiluminescent products from the ozonolysis reaction – but is consistent with the trend and
329 relative magnitudes for the substantial positive interferences shown in Tables 2 and 3. For example, a
330 lack of interference is observed for myrcene and limonene, both of which exhibit terminal C=C bonds
331 (see Table 4), and after reaction with ozone lead to the production of the CH₂OO Criegee intermediate
332 (CI) which subsequently decomposes or undergoes rearrangement to form small yields of OH (Alam *et al.*,
333 2011). The ozonolysis of internal alkenes such as cis- and trans-2-butene produce the CH₃CHOO
334 CI which predominantly decomposes via the vinyl hydroperoxide mechanism forming larger yields of
335 OH (Johnson and Marston, 2008; Alam *et al.*, 2013). Such chemically formed OH that produces a
336 detectable signal may also be augmented by contributions from HO₂ and RO₂, converted into OH within
337 the instrument by reaction with NO – especially in the NO₂ channel of photolytic converter instruments.

338
339 The relationship between the KIP (Table 4) and measured NO interference (Tables 2 and 3) is illustrated
340 in Figure 4 and can be used for predicting the potential interference of a given alkene to the NO signal
341 from a kinetic perspective. For example, α -humulene has a KIP of 94.54% which could give rise to a
342 1.7%, 2.4% or 10.2% NO interference for monitors 1, 3 and 4, respectively. This is, however, based on
343 the rate constant of α -humulene alone and does not include any structural features such as the presence
344 of terminal and non-terminal C=C bonds.

345

346

347 Explanation of the interference observed for NO₂

348

349 The above discussion considers only the interference effect arising from alkene chemiluminescent
350 emission; further measurement impacts are also evident in the (negative) interferences apparent for
351 other species / monitors in Tables 2 and 3. Inspection of Tables 2 and 3 shows smaller positive
352 interferences, and some negative interferences, from alkenes in the NO₂ measurements.

353

354 NO₂ measurements using chemiluminescence approaches are usually obtained by measuring NO_x (*i.e.*
355 $\Sigma(\text{NO} + \text{NO}_2)$), after passing the sampled air through an NO₂ converter) and subtracting the
356 (independently determined) NO contribution. If the actual interference signal (additional
357 chemiluminescence) during the NO_x measurement mode arises solely from mechanism (4), ozonolysis
358 chemiluminescence, then this would be expected to match that in the NO mode (subject to the alkene
359 abundance not being altered in the NO₂ conversion stage and if the detection conditions for the NO and
360 NO_x phases are identical), and consequently would not affect the retrieved NO₂ mixing ratio. Monitors
361 1, 2 and 3 used a single detection cell, alternating between NO and NO₂ (NO_x) modes, and so measured
362 the NO₂* chemiluminescence signal under identical conditions (optical arrangement, filtering,
363 pressure). The observed negative interference for NO₂ therefore may have arisen due to removal of
364 alkene by the Mo catalyst within the monitors.

365

366

367 For monitor 1 (TE 42i-TL), the negative interference observed for NO₂ was the same magnitude as
368 observed for the positive interference for NO, including the experiments with H₂O and CO (see Figure
369 5 and Tables 2-3). This response is thought to arise as a consequence of the calculation methodology,
370 combined with removal of alkenes during the NO₂ conversion by the Mo catalyst:

371

372 There are three modes of operation in monitor 1 (TE 42i-TL) – NO measurement, NO₂/NO_x
373 measurement and background (pre-reactor) measurement, given by Eq 1-3 respectively:

374

375



376

$$sNO = sNO_{real} + X_i \quad (\text{Eq 1})$$

$$sNOx = sNOx_{real} + yX_i \quad (\text{Eq 2})$$

$$sP = fX_i \quad (\text{Eq 3})$$

377

378 where sNO and $sNOx$ are the NO and NO_x signals produced by the chemiluminescence monitor,
 379 respectively, sNO_{real} and $sNOx_{real}$ are the ‘real’ NO and NO_x signals, X_i denotes the interference
 380 alkene i , y is the fraction of the interferant (alkene) X_i remaining after the Mo convertor, sP denotes
 381 signal at the pre-reactor and f is the fraction of X_i remaining after the pre-reactor. The mixing ratios of
 382 NO, NO₂ and NO_x are given by:
 383

$$[NO] = \frac{sNO - sP}{cNO} \quad (\text{Eq 4})$$

$$[NO] = \frac{(sNO_{real} + X_i) - fX_i}{cNO} \quad (\text{Eq 5})$$

$$[NO] = \frac{(sNO_{real} + (1 - f)X_i)}{cNO} \quad (\text{Eq 6})$$

384

$$[NOx] = \frac{sNOx - sP}{cNOx} \quad (\text{Eq 7})$$

$$[NOx] = \frac{(sNOx_{real} + yX_i) - fX_i}{cNOx} \quad (\text{Eq 8})$$

$$[NOx] = \frac{(sNOx_{real} + (y - f)X_i)}{cNOx} \quad (\text{Eq 9})$$

385

$$[NO_2] = \frac{[NOx] - [NO]}{CE} \quad (\text{Eq 10})$$

$$[NO_2] = \frac{(sNOx_{real} + (y - f)X_i)}{cNOx \times CE} - \frac{(sNO_{real} + (1 - f)X_i)}{cNO \times CE} \quad (\text{Eq 11})$$

386

387 where c is the ‘span factor’ and CE represents the conversion efficiency. If we assume $cNOx \approx cNO \approx$
 388 c , then

389

$$[NO_2] = \frac{(sNOx_{real} + (y - f)X_i) - (sNO_{real} + (1 - f)X_i)}{c \times CE} \quad (\text{Eq 12})$$

390



391 From Eq 12, it may be seen that if $y = 1$ (*i.e.* if the interferant – alkene – abundance is not affected by
392 passage through the Mo converter), then there would be no interference observed in the retrieved NO_2 ,
393 while if the interferant species is subject to removal during passage through the converter, then $y < 1$
394 and a negative interference would be observed. Molybdenum oxide catalysts have been reported to
395 efficiently isomerise alkenes at temperatures between 300 – 400 °C, (Wehrer *et al.*, 2003) and are also
396 effective catalysts for the epoxidation of alkenes (Shen *et al.*, 2019). The observed small negative
397 interference effects (for monitors 1 and 2, the Mo converter units), in the absence of significant sampled
398 NO_x , may reflect partial removal of the alkene on the converter.

399
400 The negative NO_2 interference apparent for monitors 3 and 4 (photolytic converter instruments) is more
401 difficult to rationalise (as no Mo catalyst is present). Under ambient conditions, where NO_x is present,
402 mechanism (3) may occur as outlined below. In reality, the conversion efficiency for photolytic
403 converters is substantially lower than 100% (Reed *et al.* 2016), as a consequence of both the finite
404 photolysis intensity achievable, and occurrence of the $\text{NO} + \text{O}_3$ back reaction. If the instrument
405 calibration factor for NO_x is not equal to that for NO (see Eq 11), or if alkene was removed in the
406 convertor stage, then this will lead to different interferences for NO and NO_2 , as CE is also
407 (significantly) less than 1. This trend is apparent in the values shown in Table 3, in particular for the
408 instruments fitted with photolytic converters. However, in the absence of sampled NO_x the observed
409 less-positive or even negative NO_2 interference suggests that less alkene is present in the NO_x mode.
410 Direct photolysis of alkenes is unlikely to cause such a change, considering the photolytic converter
411 wavelength envelope, but photolytic production of HO_x radicals (which then react with the alkene) may
412 be responsible.

413
414 Monitor 4 (AQD) used independent NO_2^* detection channels; tests were conducted using both channels
415 for cis-2-butene and terpinolene systems, and revealed significant differences between the two detectors
416 (*ca.* 40% lower interference response for NO in the NO_2 detection channel). With two independent
417 detection channels, NO_2 may be determined from the NO_x measurement by either subtracting the NO
418 level obtained from the NO channel (method (a)), or via the difference in signal observed in the
419 NO_2/NO_x channel when turning the photolysis lamp on and off (method (b)). Under method (a), as
420 employed for cis-2-butene and terpinolene, a lower positive interference from alkene
421 chemiluminescence results, as a consequence of the difference in the detection cell conditions (results
422 marked * in Table 3), while under method (b), as employed for the other alkenes studied here with the
423 AQD system, the interference (from mechanism 4 alone) should cancel out (results marked # in Table
424 3).

425

426 Effect of quenching by the alkenes

427

428 The data presented in Figures 1-3 and Tables 2 and 3 show both negative and positive interferences
429 while mechanism 4 alone would be expected to result in positive interference signals for NO for all
430 alkenes. We therefore conclude that additional mechanisms are occurring. Under the conditions of
431 these chamber experiments, retrieval of additional NO_y species can be precluded (the chamber wall
432 source of HONO has been characterised and shown to produce ppt levels of HONO under the dark, dry
433 conditions of these experiments (Zador *et al.*, 2005) and would be equally present for all experiments).
434 We attribute the negative (or reduced positive) interference effects to a combination of mechanisms (1)
435 and (3): quenching of excited OH (produced by alkene+ozone reaction) by alkenes – electron rich
436 alkenes have been shown to be effective quenchers (Gersdorf *et al.*, 1987; Chang and Schuster, 1987)
437 - and generation of HO_x radicals within the instrument following on from the ozonolysis reaction.

438



439 The alkene-ozone reactions are known to produce OH, HO₂ and RO₂ radicals both directly (e.g. Johnson
440 and Marston, 2008), following the photolysis of other alkene-ozone reaction products (e.g. carbonyl
441 compounds), and through OH-alkene reactions. Peroxy radicals promote the conversion of NO to NO₂,
442 altering the abundance of both species (the formation of NO_x reservoirs such as nitric acid and organic
443 nitrates will also occur, but will be negligible on the timescale of operation of most instruments).

444
445 The ozonolysis of TME results in the production of OH with close to unity yield (IUPAC, 2018) and if
446 taking into account the above mechanism (4) only, might be expected to exhibit a large interference in
447 NO mode. Table 2 shows no interference for monitors 1 and 2 (Mo convertor units) and negative and
448 positive interferences for monitors 3 and 4 (photolytic convertor units) respectively, and so is hard to
449 rationalise (for NO mode). The addition of CO as a scavenger for OH led to an increase in the NO signal
450 for all monitors. A possible origin of this signal is the production of the excited intermediate HOCO
451 (from reaction of vibrationally excited OH, from the ozonolysis of TME, with CO), which has a
452 temperature and pressure dependent rate of reaction, (Atkinson *et al.*, 2006; Li and Francisco, 2000)
453 and is consistent with the larger NO signal in the photolytic monitors (Table 2).

454

455 CONCLUSION

456

457 The interference in chemiluminescence NO_x measurements from alkenes has been systematically
458 investigated using four commercially available monitors. There are varying degrees of interferences in
459 the NO and NO₂ signals by all monitors investigated and are due to a combination of mechanisms 1, 3
460 and 4. Monoterpenes, α -terpinene and terpinolene, exhibit the largest interferences followed by 2,3-
461 dimethyl-2-butene (TME) and trans-2-butene, in line with the calculated KIP (see Table 4). The KIP
462 can be used as a crude indicator for a potential interference of an alkene to a NO signal, but have large
463 margins of error as they do not take into account the variation in the yield of chemiluminescent products
464 and other instrumental differences. The alkene interference observed with enhanced RH conditions also
465 indicates the need to accurately calibrate chemiluminescence NO_x analysers under actual sampling
466 conditions.

467

468 The NO interferences from alkenes among the monitors investigated in this study ranges from 1 to 11%.
469 The varying responses exhibited by the different monitors reflect differences in the conditions within
470 the instrument (ozone abundance, pressure and residence time) within the reaction cell and filter
471 specifications. The magnitude of the NO and NO₂ interferences not only vary with different alkenes
472 and commercial monitors, but will also be dependent upon sampling environments (and with trends in
473 ambient NO_x and alkenes). Notably, in these experiments the alkene abundance is high compared with
474 most ambient air samples – consequently internally generated OH will react essentially exclusively with
475 the alkene, which may not reflect ambient sampling – but which we do not expect to impact the
476 conclusions reached with respect to mechanism 4, interference in retrieved NO levels. Further research
477 to explore these impacts, and other parameters (e.g. H₂O abundance), is urgently needed.

478

479 Mixing ratios of NO_x vary from > 100 ppb in some urban areas, e.g. Marylebone Road (Carslaw *et al.*
480 2005), < 300 ppt in biogenic environments (Hewitt *et al.* 2010) and < 35 ppt in remote areas (Lee *et al.*
481 2009). For typical urban environments where alkene mixing ratios are relatively low (< 2 ppb e.g. von
482 Schneidmesser *et al.* 2010) these interferences are not likely to be significant (~ 1% of the NO signal).
483 However, for biogenic environments where monoterpenes and sesquiterpenes, which react rapidly with
484 ozone, are abundant, this interference could be significantly larger. For example, average mixing ratios
485 for isoprene (~ 1 ppb), 5 monoterpenes (~ 220 ppt), 3 short chain alkenes (~ 240 ppt) and NO (0.14
486 ppb) were measured within a south-east Asian tropical rainforest (Jones *et al.*, 2011). Using the



487 relationship between KIP and NO interference an overestimation of NO levels of to up to 58% may be
488 observed, with very significant implications for prediction of other atmospheric chemical processes
489 involving NO_x. Given that NO_x mixing ratios are relatively small in biogenic and remote environments,
490 these interferences could lead to a substantial overestimation. Alkene interference contribute to the
491 relatively high NO and low NO₂ reported in the tropical rainforest at night, which could not be otherwise
492 accounted for (Pugh *et al.* 2011).

493

494 Within indoor environments, NO_x primarily arises from outdoor sources or indoor combustion sources
495 (Young *et al.*, 2019). Typically, in the absence of a known indoor combustion source, indoor NO levels
496 are low (*ca.* 13% of outdoor levels) with NO₂ comprising the majority of the NO_x (Zhou *et al.*, 2019). ,
497 There are multiple sources of alkene indoors, such as fragranced volatile personal care products
498 (Nemafollahi *et al.*, 2019; Yeoman *et al.*, 2020) and cleaning products (Kristenson *et al.*, 2019),
499 resulting in very much larger levels than NO_x (McDonald *et al.*, 2018; Kristenson *et al.*, 2019).
500 Consequently, monoterpenes are among the most ubiquitous VOC reported for indoor air, with the main
501 species including, linalool, α -pinene, β -myrcene and limonene (Krol *et al.* 2014; Nematollahi *et al.* 2019).
502 Monoterpene mixing ratios in indoor environments are reported to be 5 to 7 times larger than those
503 reported outdoors (low ppb levels), and can be further enhanced by cleaning activities (Singer *et al.*,
504 2006; Kristenson *et al.*, 2019; Weschler and Carslaw, 2018). Peak limonene mixing ratios may be a
505 factor of *ca.* 50 higher indoors than outdoor environments (Colman Lerner *et al.*, 2012), while indoor
506 α -terpinene and α -pinene mixing ratios have exceeded 10 and 68 ppb, respectively (Singer *et al.*, 2006;
507 Brown *et al.*, 1994). These relatively large monoterpene ratios may lead to substantial interferences in
508 chemiluminescence NO_x monitors; their incorrect retrieval as measured “NO_x” will impact assessments
509 of indoor air quality and health.

510

511 DATA AVAILABILITY.

512 Experimental data will be available in the Eurochamp database, www.eurochamp.org, from the
513 H2020 EUROCHAMP2020 project, GA no. 730997

514

515 AUTHOR CONTRIBUTIONS

516 MSA, WJB and JDL conceived and planned the experiments. MSA, JDL, MV, AM and MR performed
517 the experiments. LRC, LJK and MSA performed the data analysis. LRC, LJK, MSA, CF and WJB
518 contributed to data investigation and curation. MSA wrote the original draft manuscript and all co-
519 authors contributed to reviewing and editing the paper.

520

521 COMPETING INTERESTS

522 The authors declare that they have no conflict of interest.

523

524 ACKNOWLEDGEMENTS

525 This work was funded in part through the UK Natural Environment Research Council (NERC) project
526 “ICOZA: Integrated Chemistry of Ozone in the Atmosphere” (NE/ K012169/1) and by the
527 EUROCHAMP-2 Transnational access project “NOxINT: NOx analyser interference in chemically
528 complex mixtures” (E2-2010-05-26-0033) . Part of this work has received funding from the European
529 Union’s Horizon 2020 research and innovation programme through the EUROCHAMP-2020
530 Infrastructure Activity under grant agreement No. 730997. CEAM is partly supported by the
531 IMAGINA-Prometeo project (PROMETEO2019/110) and by Generalitat Valenciana. In addition, we
532 thank Eva Clemente for their work in these experiments.

533

534

535



536 **REFERENCES**

537

538 Alam, M. S., Camredon, M., Rickard, A. R., Carr, T., Wyche, K. P., Hornsby, K. E., Monks, P. S., and
539 Bloss, W. J.: Total radical yields from tropospheric ethene ozonolysis, *Phys Chem Chem Phys*, 13,
540 11002-11015, 2011.

541

542 Alam, M. S., Rickard, A. R., Camredon, M., Wyche, K. P., Carr, T., Hornsby, K. E., Monks, P. S., and
543 Bloss, W. J.: Radical product yields from the ozonolysis of short chain alkenes under atmospheric
544 boundary layer conditions, *J Phys Chem A*, 117, 12468-12483, 2013.

545

546 Atkinson, R., Baulch, D.L., Cox, R.A., Crowley, J.N., Hampson, R.F., Hynes, R.G., Jenkin, M.E.,
547 Rossi, M.J. and Troe, J.: Evaluated kinetic and photochemical data for atmospheric chemistry: Volume
548 II – gas phase reactions of organic species, *Atmos. Chem. Phys.*, 6, 3625-4055, 2006.

549

550 AQEG: Air quality expert group. Nitrogen dioxide in the United Kingdom, 2004.

551

552 Brown, S.K., Sim, M.R., Abramson, M.J. and Gray, C.N.: Concentrations of volatile organic
553 compounds in indoor air—a review, *Indoor air*, 4, 2, 123-134, 1994

554 BS EN 14211: Ambient air. Standard method for the measurement of the concentration of nitrogen
555 dioxide and nitrogen monoxide by chemiluminescence, The British Standards Institution, 2012

556

557 Cape, J. N.: The Use of Passive Diffusion Tubes for Measuring Concentrations of Nitrogen Dioxide in
558 Air, *Critical Reviews in Analytical Chemistry*, 39, 289-310, 2009.

559

560 Carslaw, D. C.: Evidence of an increasing NO₂/NO_x emissions ratio from road traffic emissions,
561 *Atmospheric Environment*, 39, 4793-4802, 2005.

562

563 Carslaw, D. C. and Rhys-Tyler, G.: New insights from comprehensive on-road measurements of NO_x,
564 NO₂ and NH₃ from vehicle emission remote sensing in London, UK, *Atmospheric Environment*, 81,
565 339-347, 2013.

566

567 Chaloulakou, A., Mavroidis, I., and Gavriil, I.: Compliance with the annual NO₂ air quality standard in
568 Athens. Required NO_x levels and expected health implications, *Atmospheric Environment*, 42, 454-
569 465, 2008.

570

571 Chang, S. L. P. and Schuster, D. I.: Fluorescence quenching of 9,10-dicyanoanthracene by dienes and
572 alkenes, *The Journal of Physical Chemistry*, 91, 3644-3649, 1987.

573

574 Crawford, J., Davis, D., Chen, G., Bradshaw, J., Sandholm, S., Kondo, Y., Merrill, J., Liu, S., Browell,
575 E., and Gregory, G.: Implications of large scale shifts in tropospheric NO_x levels in the remote tropical
576 Pacific, *Journal of Geophysical Research: Atmospheres*, 102, 28447-28468, 1997.

577

578 Dillon, T. J. and Crowley, J. N.: Reactive quenching of electronically excited NO₂* and NO₃* by H₂O
579 as potential sources of atmospheric HO_x radicals, *Atmos. Chem. Phys.*, 18, 14005-14015, 2018.

580

581 Dunlea, E. J., Herndon, S. C., Nelson, D. D., Volkamer, R. M., San Martini, F., Sheehy, P. M., Zahniser,
582 M. S., Shorter, J. H., Wormhoudt, J. C., Lamb, B. K., Allwine, E. J., Gaffney, J. S., Marley, N. A.,



- 583 Grutter, M., Marquez, C., Blanco, S., Cardenas, B., Retama, A., Ramos Villegas, C. R., Kolb, C. E.,
584 Molina, L. T., and Molina, M. J.: Evaluation of nitrogen dioxide chemiluminescence monitors in a
585 polluted urban environment, *Atmos. Chem. Phys.*, 7, 2691-2704, 2007.
- 586
- 587 European Environmental Agency.: Air quality in Europe - 2018 report, ISSN 1997-8449, Report No:
588 TH-AL-18-013-EN-N, 2018.
- 589
- 590 Finlayson, B., Pitts Jr, J., and Atkinson, R.: Low-pressure gas-phase ozone-olefin reactions.
591 Chemiluminescence, kinetics, and mechanisms, *Journal of the American Chemical Society*, 96, 5356-
592 5367, 1974.
- 593
- 594 Fuchs, H., Dubé, W. P., Lerner, B. M., Wagner, N. L., Williams, E. J., and Brown, S. S.: A sensitive
595 and versatile detector for atmospheric NO₂ and NO_x based on blue diode laser cavity ring-down
596 spectroscopy, *Environmental science & technology*, 43, 7831-7836, 2009.
- 597
- 598 Gerboles, M., Lagler, F., Rembges, D., and Brun, C.: Assessment of uncertainty of NO₂ measurements
599 by the chemiluminescence method and discussion of the quality objective of the NO₂ European
600 Directive, *Journal of Environmental Monitoring*, 5, 529-540, 2003.
- 601
- 602 Gersdorf, J., Mattay, J., and Goerner, H.: Photoreactions of biacetyl, benzophenone, and benzil with
603 electron-rich alkenes, *J. Am. Chem. Soc.*; (United States), 1987. Medium: X; Size: Pages: 1203-1209,
604 1987.
- 605
- 606 Goldstein, A. H. and Galbally, I. E.: Known and Unexplored organic constituents in the Earth's
607 Atmosphere, *Environmental Science and Technology*, 2007. 1515-1521, 2007.
- 608
- 609 Grice, S., Stedman, J., Kent, A., Hobson, M., Norris, J., Abbott, J., and Cooke, S.: Recent trends and
610 projections of primary NO₂ emissions in Europe, *Atmospheric Environment*, 43, 2154-2167, 2009.
- 611
- 612 Hansen, D., Atkinson, R., and Pitts Jr, J.: Structural effects on the chemiluminescence from the reaction
613 of ozone with selected organic compounds, *Journal of Photochemistry*, 7, 379-404, 1977.
- 614
- 615 Heard, D.: Analytical techniques for atmospheric measurement, John Wiley & Sons, 2008.
- 616
- 617 Hewitt, C. N., Lee, J. D., MacKenzie, A. R., Barkley, M. P., Carslaw, N., Carver, G. D., Chappell, N.
618 A., Coe, H., Collier, C., Commane, R., Davies, F., Davison, B., DiCarlo, P., Di Marco, C. F., Dorsey,
619 J. R., Edwards, P. M., Evans, M. J., Fowler, D., Furneaux, K. L., Gallagher, M., Guenther, A., Heard,
620 D. E., Helfter, C., Hopkins, J., Ingham, T., Irwin, M., Jones, C., Karunaharan, A., Langford, B., Lewis,
621 A. C., Lim, S. F., MacDonald, S. M., Mahajan, A. S., Malpass, S., McFiggans, G., Mills, G., Misztal,
622 P., Moller, S., Monks, P. S., Nemitz, E., Nicolas-Perea, V., Oetjen, H., Oram, D. E., Palmer, P. I.,
623 Phillips, G. J., Pike, R., Plane, J. M. C., Pugh, T., Pyle, J. A., Reeves, C. E., Robinson, N. H., Stewart,
624 D., Stone, D., Whalley, L. K., and Yin, X.: Overview: oxidant and particle photochemical processes
625 above a south-east Asian tropical rainforest (the OP3 project): introduction, rationale, location
626 characteristics and tools, *Atmos. Chem. Phys.*, 10, 169-199, 2010.
- 627
- 628 Hills, A. J. and Zimmerman, P. R.: Isoprene measurement by ozone-induced chemiluminescence,
629 *Analytical Chemistry*, 62, 1055-1060, 1990.
- 630



- 631 Johnson, D. and Marston, G.: The gas-phase ozonolysis of unsaturated volatile organic compounds in
632 the troposphere, *Chem Soc Rev*, 37, 699-716, 2008.
- 633
- 634 Jones, C.E., Hopkins, J.R. and Lewis, A.C.: In situ measurements of isoprene and monoterpenes
635 within a south-east Asian tropical rainforest, *Atmospheric chemistry and Physics*, 11, 14, 6971, 2011
- 636 Kasyutich, V.L., Bale, C.S.E., Canosa-Mas, C.E., Pfrang, C., Vaughan, S. and Wayne, R.P.: Cavity-
637 enhanced absorption: detection of nitrogen dioxide and iodine monoxide using a violet laser diode,
638 *Applied Physics B*, 76, 691-697, 2003.
- 639
- 640 Kebabian, P. L., Herndon, S. C., and Freedman, A.: Detection of Nitrogen Dioxide by Cavity Attenuated
641 Phase Shift Spectroscopy, *Analytical Chemistry*, 77, 724-728, 2005.
- 642
- 643 Keuken, M., Roemer, M., and van den Elshout, S.: Trend analysis of urban NO₂ concentrations and the
644 importance of direct NO₂ emissions versus ozone/NO_x equilibrium, *Atmospheric Environment*, 43,
645 4780-4783, 2009.
- 646
- 647 Kristensen, K., Lunderberg, D. M., Liu, Y., Misztal, P.K., Tian, Y., Arata, C., Nazaroff, W. W. and
648 Goldstein, A.H.: Sources and dynamics of semivolatile organic compounds in a single-family residence
649 in northern California. *Indoor Air*, 29, 4, 645-655, 2019.
- 650
- 651 Król, S., Namieśnik, J. and Zabiegała, B.: α -Pinene, 3-carene and d-limonene in indoor air of Polish
652 apartments: The impact on air quality and human exposure. *Science of the total environment*, 468, 985-
653 995, 2014.
- 654
- 655 Lamsal, L., Martin, R., Van Donkelaar, A., Steinbacher, M., Celarier, E., Bucsela, E., Dunlea, E., and
656 Pinto, J.: Ground-level nitrogen dioxide concentrations inferred from the satellite-borne Ozone
657 Monitoring Instrument, *Journal of Geophysical Research: Atmospheres*, 113, 2008.
- 658
- 659 Lee, J. D., Moller, S. J., Read, K. A., Lewis, A. C., Mendes, L., and Carpenter, L. J.: Year-round
660 measurements of nitrogen oxides and ozone in the tropical North Atlantic marine boundary layer,
661 *Journal of Geophysical Research: Atmospheres*, 114, 2009.
- 662
- 663 Lerner, J.C., Sanchez, E.Y., Sambeth, J.E. and Porta, A.A.: Characterization and health risk
664 assessment of VOCs in occupational environments in Buenos Aires, Argentina, *Atmospheric*
665 *environment*, 55, 440-447, 2012.
- 666
- 666 Li, Y. and Francisco, J.S.: High level ab initio studies on the excited states of HOCO radical. *The*
667 *Journal of Chemical Physics*, 113, 18, 7963-7970, 2000
- 668
- 669 Matthews, R. D., Sawyer, R. F., and Schefer, R. W.: Interferences in chemiluminescent measurement
670 of nitric oxide and nitrogen dioxide emissions from combustion systems, *Environmental Science &*
671 *Technology*, 11, 1092-1096, 1977.
- 672
- 673 McDonald, B.C., de Gouw, J.A., Gilman, J.B., Jathar, S.H., Akherati, A., Cappa, C.D., Jimenez, J.L.,
674 Lee-Taylor, J., Hayes, P.L., McKeen, S.A. and Cui, Y.Y.: Volatile chemical products emerging as
675 largest petrochemical source of urban organic emissions, *Science*, 359, 6377, 760-764, 2018.
- 676



- 677 Muñoz, A., Vera, T., Sidebottom, H., Mellouki, A., Borrás, E., Ródenas, M., Clemente, E., and
678 Vázquez, M.: Studies on the Atmospheric Degradation of Chlorpyrifos-Methyl, *Environmental Science
679 & Technology*, 45, 1880-1886, 2011.
680
- 681 Murphy, J. G., Day, D. A., Cleary, P. A., Wooldridge, P. J., Millet, D. B., Goldstein, A. H., and Cohen,
682 R. C.: The weekend effect within and downwind of Sacramento – Part 1: Observations of ozone,
683 nitrogen oxides, and VOC reactivity, *Atmos. Chem. Phys.*, 7, 5327-5339, 2007.
684
- 685 Navas, M. J., Jiménez, A. M., and Galán, G.: Air analysis: determination of nitrogen compounds by
686 chemiluminescence, *Atmospheric Environment*, 31, 3603-3608, 1997.
687
- 688 Nematollahi, N., Kolev, S. D. and Steinemann, A.: Volatile chemical emissions from 134 common
689 consumer products. *Air Quality, Atmosphere & Health*, 12, 11, 1259-1265, 2019.
690
- 691 Pugh, T. A. M., Ryder, J., MacKenzie, A. R., Moller, S. J., Lee, J. D., Helfter, C., Nemitz, E., Lowe,
692 D., and Hewitt, C. N.: Modelling chemistry in the nocturnal boundary layer above tropical rainforest
693 and a generalised effective nocturnal ozone deposition velocity for sub-ppbv NO_x conditions, *Journal
694 of Atmospheric Chemistry*, 65, 89-110, 2010.
695
- 696 Reed, C., Evans, M. J., Di Carlo, P., Lee, J. D., and Carpenter, L. J.: Interferences in photolytic NO₂
697 measurements: explanation for an apparent missing oxidant?, *Atmos. Chem. Phys.*, 16, 4707-4724,
698 2016.
699
- 700 Sandholm, S., Bradshaw, J., Dorris, K., Rodgers, M., and Davis, D.: An airborne compatible
701 photofragmentation two-photon laser-induced fluorescence instrument for measuring background
702 tropospheric levels of NO, NO_x, and NO₂, *Journal of Geophysical Research: Atmospheres*, 95, 10155-
703 10161, 1990.
704
- 705 Schurath, U., Guesten, H., and Penzhorn, R.-D.: Phosphorescence of α -diketones from ozone-olefin
706 reactions, *Journal of Photochemistry*, 5, 33-40, 1976.
707
- 708 Shen, Y., Jiang, P., Wai, P. T., Gu, Q., and Zhang, W.: Recent Progress in Application of Molybdenum-
709 Based Catalysts for Epoxidation of Alkenes, *Catalysts*, 9, 31, 2019.
710
- 711 Shrivastava, M., Cappa, C. D., Fan, J., Goldstein, A. H., Guenther, A. B., Jimenez, J. L., Kuang, C.,
712 Laskin, A., Martin, S. T., and Ng, N. L.: Recent advances in understanding secondary organic aerosol:
713 Implications for global climate forcing, *Reviews of Geophysics*, 55, 509-559, 2017.
714
- 715 Singer, B.C., Coleman, B.K., Destailats, H., Hodgson, A.T., Lunden, M.M., Weschler, C.J. and
716 Nazaroff, W.W.: Indoor secondary pollutants from cleaning product and air freshener use in the
717 presence of ozone, *Atmospheric Environment*, 40, 35, 6696-6710, 2006.
- 718 Steinbacher, M., Zellweger, C., Schwarzenbach, B., Bugmann, S., Buchmann, B., Ordonez, C., Prévôt,
719 A. S., and Hueglin, C.: Nitrogen oxide measurements at rural sites in Switzerland: Bias of conventional
720 measurement techniques, *Journal of Geophysical Research: Atmospheres*, 112, 2007.
721
- 722 Toby, S.: Chemiluminescence in the reactions of ozone, *Chemical Reviews*, 84, 277-285, 1984.
723



- 724 USEPA: Quality assurance handbook. Reference method for determination of nitrogen dioxide in the
725 atmosphere (chemiluminescence), 2.3, 2, 2002.
726
- 727 Velasco, E., Lamb, B., Westberg, H., Allwine, E., Sosa, G., Arriaga-Colina, J. L., Jobson, B. T.,
728 Alexander, M. L., Prazeller, P., Knighton, W. B., Rogers, T. M., Grutter, M., Herndon, S. C., Kolb, C.
729 E., Zavala, M., de Foy, B., Volkamer, R., Molina, L. T., and Molina, M. J.: Distribution, magnitudes,
730 reactivities, ratios and diurnal patterns of volatile organic compounds in the Valley of Mexico during
731 the MCMA 2002 & 2003 field campaigns, *Atmos. Chem. Phys.*, 7, 329-353, 2007.
732
- 733 Villena, G., Bejan, I., Kurtenbach, R., Wiesen, P., and Kleffmann, J.: Development of a new Long Path
734 Absorption Photometer (LOPAP) instrument for the sensitive detection of NO₂ in the atmosphere,
735 *Atmospheric Measurement Techniques Discussions*, 4, 1751-1793, 2011.
736
- 737 Villena, G., Bejan, I., Kurtenbach, R., Wiesen, P., and Kleffmann, J.: Interferences of commercial NO₂
738 instruments in the urban atmosphere and in a smog chamber, *Atmos. Meas. Tech.*, 5, 149-159, 2012.
739
- 740 von Schneidmesser, E., Monks, P. S., and Plass-Duelmer, C.: Global comparison of VOC and CO
741 observations in urban areas, *Atmospheric Environment*, 44, 5053-5064, 2010.
742
- 743 Wehrer, P., Libs, S., and Hilaire, L.: Isomerization of alkanes and alkenes on molybdenum oxides,
744 *Applied Catalysis A: General*, 238, 69-84, 2003.
745
- 746 Weschler, C.J. and Carslaw, N.: Indoor chemistry, *Environ. Sci. Technol*, 52, 2419–2428, 2018.
- 747 Wiesen, P.: Photooxidant Studies Using the European Photoreactor EUPHORE, Berlin, Heidelberg,
748 2001, 155-162.
749
- 750 Yeoman, A. M., Shaw, M., Carslaw, N., Murrells, T., Passant, N., Lewis, A. C.: Simplified speciation
751 and atmospheric volatile organic compounds emission rates from non-aerosol personal care products.
752 *Indoor Air*, 0, 1– 14, 2020
753
- 754 Young, C.J., Zhou, S., Siegel, J.A. and Kahan, T.F.: Illuminating the dark side of indoor oxidants.
755 *Environmental Science: Processes & Impacts*, 21, 8, 1229-1239, 2019.
756
- 757 Zhou, S., Young, C. J., VandenBoer, T. C. and Kahan, T. F.: Role of location, season, occupant activity,
758 and chemistry in indoor ozone and nitrogen oxide mixing ratios. *Environmental Science: Processes &
759 Impacts*, 21, 8, 1374-1383, 2019.
760
761
762
763
764
765
766
767
768
769
770



771

772

773 **Table 1:** Details of the NO_x monitoring instruments used.

Number	Manufacturer	Model	Institution	NO ₂ Convertor	Limit of Detection (LOD)*	
					NO (ppt)	NO ₂ (ppt)
1	Thermo	TE42i-TL	Birmingham	Heated Mo	210	210
2	API	200AU	EUPHORE	Heated Mo	190	450
3	Eco Physics	CLD 770 Alppt / PLC 760	EUPHORE	Xe lamp	150	430
4	Air Quality Designs	-	York	Blue light at 395 nm	60	150

*Calculated in this study

774

775

776

777

778

779

780

781

782

783

784

785

786

787

788

789

790

791

792

793

794

795

796

797

798

799

800

801

802

803

804

805

806



807

808

809 **Table 2:** Measured NO interference ($\% \pm 1$ s.d. of the slope) for each monitor across a range of different
 810 alkenes (LOD: Limit of Detection).

<i>Species</i>	<i>1: TE 42i-TL</i>	<i>2: API 200AU</i>	<i>3: Eco Physics CLD770</i>	<i>4: Air Quality Designs</i>
cis-2-butene	< LOD	< LOD	0.4 ± 0.05	0.38 ± 0.004
TME	< LOD	< LOD	-0.7 ± 0.09	1.1 ± 0.001
Trans-2-butene	< LOD	< LOD	1.0 ± 0.008	0.83 ± 0.01
Terpinolene	0.5 ± 0.05	< LOD	1.3 ± 0.01	4.4 ± 0.15
α-Terpinene	1.9 ± 0.05	0.5 ± 0.04	2.3 ± 0.04	10.9 ± 0.06
Limonene	< LOD	< LOD	< LOD	-0.10 ± 0.001
TME + H ₂ O	< LOD	< LOD	0.6	2.4
Trans-2-butene + H ₂ O	< LOD	< LOD	0.48 ± 0.006	0.37 ± 0.01
Terpinolene + H ₂ O	0.25 ± 0.03	< LOD	0.88 ± 0.004	1.6 ± 0.1
α-Terpinene + H ₂ O	1.0 ± 0.07	< LOD	1.3 ± 0.06	6.2 ± 0.7
TME + CO	0.70 ± 0.002	0.66 ± 0.09	1.3 ± 0.12	1.4 ± 0.02

811

812

813

814

815

816

817

818

819

820

821

822

823

824

825

826

827

828

829

830

831

832

833

834

835

836

837

838

839

840

841



842

843

844 **Table 3:** Measured NO_2 interference ($\% \pm 1$ s.d. of the slope) for each monitor across a range of
 845 different alkenes (LOD: Limit of Detection).

<i>Species</i>	<i>1: TE 42i-TL</i>	<i>2: API 200AU</i>	<i>3: Eco Physics CLD770</i>	<i>4: Air Quality Designs</i>
cis-2-butene	-0.6 ± 0.1	< LOD	-1.1 ± 0.08	0.3 ± 0.02
TME	-0.63 ± 0.05	< LOD	-0.78 ± 0.15	-0.92 ± 0.1
Trans-2-butene	-0.5 ± 0.06	< LOD	-0.5 ± 0.03	-0.93 ± 0.02
Terpinolene	-0.61 ± 0.02	< LOD	-0.18 ± 0.03	1.6 ± 0.1
α -Terpinene	-1.9 ± 0.13	< LOD	-1.0 ± 0.2	3.1 ± 2.1
Limonene	< LOD	< LOD	< LOD	0.09 ± 0.003
TME + H ₂ O	-0.6	< LOD	< LOD	-2.0
Trans-2-butene + H ₂ O	< LOD	< LOD	< LOD	-0.41 ± 0.02
Terpinolene + H ₂ O	-0.29 ± 0.02	< LOD	< LOD	-0.25
α -Terpinene + H ₂ O	-0.98 ± 0.06	< LOD	< LOD	0.35 ± 0.1
TME + CO	-0.70 ± 0.01	< LOD	< LOD	1.0 ± 0.3

846

847

848

849

850

851

852

853

854

855

856

857

858

859

860

861

862

863

864

865

866

867

868

869

870

871

872

873

874

875

876



877

878

879

880 **Table 4:** Kinetic ranking of interference potential: the percentage of the potential chemiluminescent
 881 signal from ozonolysis of a given alkene which would not be removed by a standard instrument
 882 background cycle, under conditions (ozone mixing ratio, residence time) which would remove 99% of
 883 the NO sampled. Rate constants are taken from Calvert et al. (2000). NB: this ranking does not include
 884 variations in the yield of chemiluminescent products with alkene structure, which will modulate the
 885 values given. Species marked * are investigated in this study.

886

Species	$k_{(\text{Alkene}+\text{O}_3)}(298\text{ K})$ /cm ³ molecule ⁻¹ s ⁻¹	Kinetic Interference Potential (%)	No. of C=C bonds	No. of terminal C=C bonds
Ethene	1.58×10^{-18}	0.04 *	1	1
1-Butene	9.64×10^{-18}	0.23	1	1
2,3-dimethyl-1-butene	1.00×10^{-17}	0.24	1	1
Propene	1.01×10^{-17}	0.24 *	1	1
1-pentene	1.06×10^{-17}	0.26	1	1
Isobutene	1.13×10^{-17}	0.27 *	1	1
Isoprene	1.28×10^{-17}	0.31 *	1	1
2-methyl-1-butene	1.30×10^{-17}	0.31	1	1
β-pinene	1.50×10^{-17}	0.36 *	1	1
α-cedrene	2.80×10^{-17}	0.68	1	0
3-carene	3.70×10^{-17}	0.89	1	0
α-pinene	8.66×10^{-17}	2.08 *	1	0
cis-2-butene	1.25×10^{-16}	2.98 *	1	0
cis-3-hexane	1.44×10^{-16}	3.43	1	0
trans-3-hexane	1.57×10^{-16}	3.73	1	0
α-coapene	1.58×10^{-16}	3.76	1	0
trans-2-butene	1.90×10^{-16}	4.50 *	1	0
Limonene	2.00×10^{-16}	4.73 *	2	1
2-carene	2.30×10^{-16}	5.42	1	0
2-methyl-2-butene	4.03×10^{-16}	9.31	1	0
Myrcene	4.70×10^{-16}	10.77 *	3	2
2,3-dimethyl-2-butene	1.13×10^{-15}	23.96 *	1	0
Terpinolene	1.90×10^{-15}	36.90 *	2	0
α-humulene	1.20×10^{-14}	94.54	3	0
β-carophyllene	1.20×10^{-14}	94.54	2	1
α-terpinene	2.10×10^{-14}	99.38 *	2	0

887

888

889

890

891

892

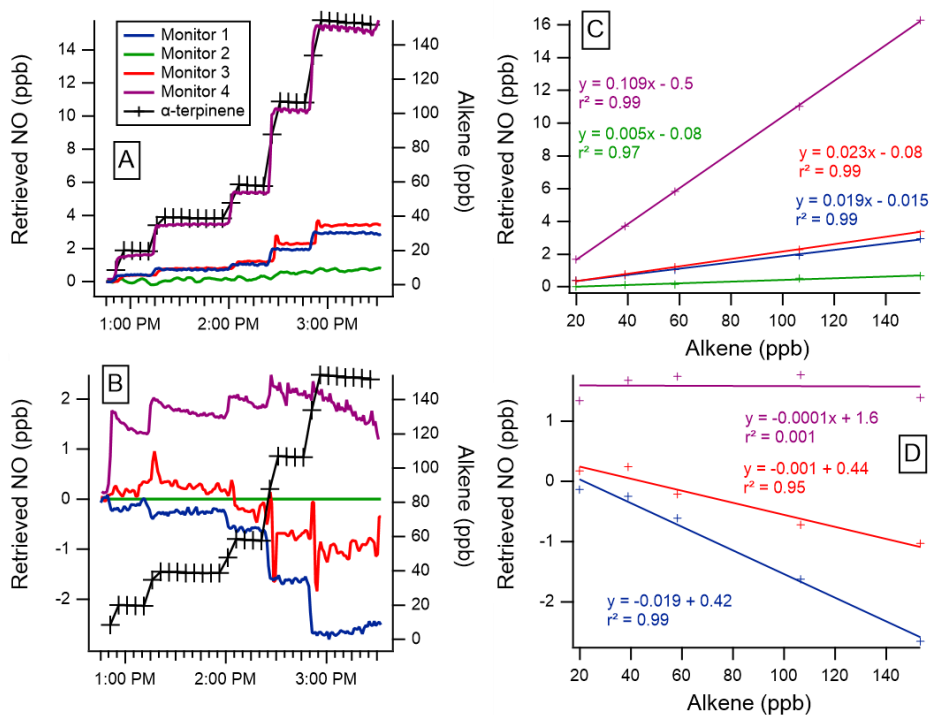
893

894

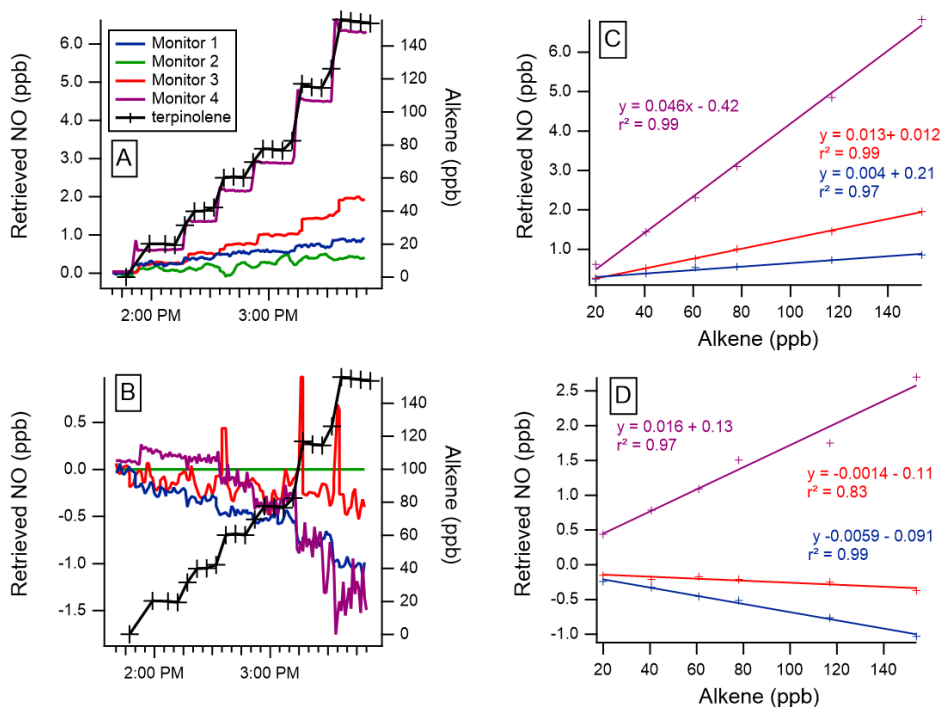
895



896
897
898
899



900
901 **Figure 1:** Time series of the α -terpinene mixing ratio and indicated / “measured” NO (top) and NO₂
902 (bottom) mixing ratios as directly retrieved by each monitor (left column) and the regression
903 calculations for the monitors that demonstrated significant interference with the addition of α -
904 terpinene (right column). Note the different y-axis scales.
905
906
907

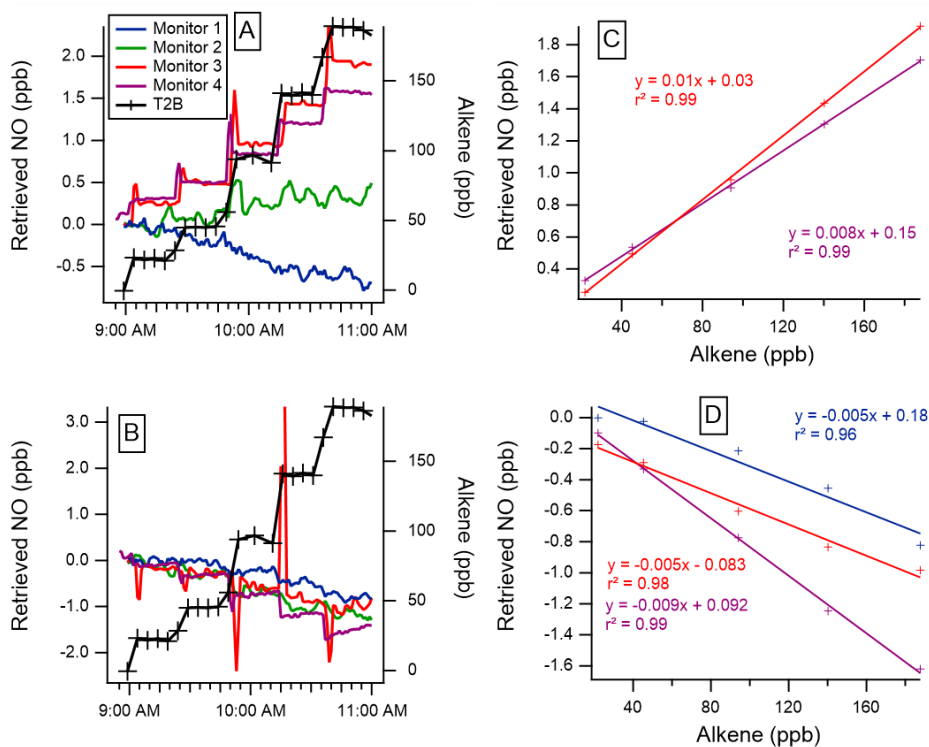


908
909
910
911
912
913

Figure 2: Time series of the terpinolene mixing ratio and measured NO and NO₂ mixing ratios as retrieved by each monitor (left column) and the regression calculations for the monitors that demonstrated significant interference with the addition of terpinolene (right column). Note the different y-axis scales.



914

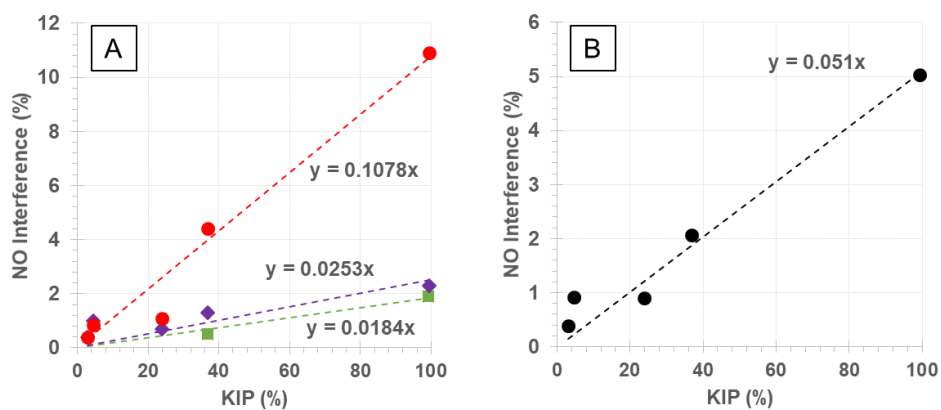


915
916
917
918
919
920
921

Figure 3: Time series of the trans-2-butene (T2B) mixing ratio and measured NO (top) and NO₂ (bottom) mixing ratios as retrieved by each monitor (left column) and the regression calculations for the monitors that demonstrated significant interference with the addition of T2B (right column). Note the different y-axis scales.



922
923

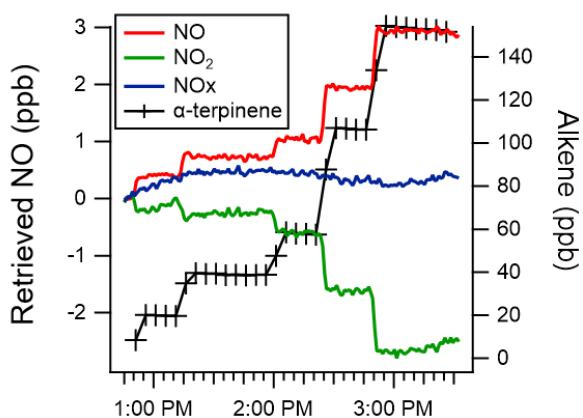


924
925
926
927
928
929
930
931
932
933
934
935
936
937
938
939
940
941
942
943
944
945
946
947
948
949
950
951
952
953
954

Figure 4: Relationship between measured NO interference (%) and kinetic interference potential, KIP (%) for monitors 1 (green), 3 (purple), 4 (red) and the average of the observed NO interference across all instruments (black).



955
956



957
958 **Figure 5:** Time series of the α -terpinene mixing ratio (black) and measured NO (red), NO₂ (green) and
959 NO_x (blue) mixing ratios as retrieved by monitor 1 (TE 42i-TL).
960
961
962
963
964
965
966
967
968
969
970
971
972